Results in Physics 20 (2021) 103663

Contents lists available at ScienceDirect

Results in Physics

journal homepage: www.elsevier.com/locate/rinp

New applications related to Covid-19

Ali Akgül [a,*], Nauman Ahmed [b,d], Ali Raza [c], Zafar Iqbal [b,d], Muhammad Rafiq [e], Dumitru Baleanu [f,g,h], Muhammad Aziz-ur Rehman [b]

[a] Siirt University, Art and Science Faculty, Department of Mathematics, TR-56100 Siirt, Turkey
[b] University of Management and Technology, Lahore, Pakistan, The University of Lahore, Lahore, Pakistan
[c] Faculty of Computing, National College of Business Administration and Economics, Lahore, Pakistan
[d] Department of Mathematics and statistics, The University of Lahore, Lahore, Pakistan
[e] Department of Mathematics, Faculty of Sciences, University of Central Punjab, Lahore, Pakistan
[f] Department of Mathematics, Cankaya University, 06530 Balgat, Ankara, Turkey
[g] Institute of Space Sciences, R76900 Magurele-Bucharest, Romania
[h] Department of Medical Research, China Medical University, Taichung 40402, Taiwan

ARTICLE INFO

Keywords:
Covid-19
Fractal fractional derivative
Stability analysis
Numerical simulations

ABSTRACT

Analysis of mathematical models projected for COVID-19 presents in many valuable outputs. We analyze a model of differential equation related to Covid-19 in this paper. We use fractal-fractional derivatives in the proposed model. We analyze the equilibria of the model. We discuss the stability analysis in details. We apply very effective method to obtain the numerical results. We demonstrate our results by the numerical simulations.

Introduction

Working the concept of disease invention and diffusion has been presented in [1]. The invention of diseases and epidemics has been taken an excellent interest by many investigators [2]. The fractional calculus has been enhanced recently to investigate the new problems [3]. Additionally, more knowledge and definitions have been presented in [4–6]. Fractional calculus generalize the differentiation and integration of integer order to real or fractional order [7]. Recently, many new operators have been defined related to the fractional differential equations.

Corona viruses are a wide family of viruses that have a typical corona. They were named corona viruses in 1960 because of their view. Viruses that give rise routine cold diseases and fatal diseases, such as Middle East respiratory syndrome (MERS-CoV) and severe acute respiratory syndrome (SARS-CoV), are from the corona viruses family. The researchers have obtained that the corona viruses are conducted between animals and people. Additionally, many corona viruses that have not yet infected humans are circulating in animals [8]. Many investigators concentrated this urgent topic nowadays [9–12]. This wide research will allow the human kind to apply a robust and fast response to a problem that is causing a severe global socioeconomic disruption [13]. For more details see [19–22].

The main goal of this paper is to analyse and obtain the solution for the system of nonlinear ordinary differential equations defining the deadly and most dangerous virus.

Preliminaries

Definition 0.1. We suppose that $u(t)$ is continuous in (a,b) and fractal differentiable on (a,b) with order θ. Then, the fractal-fractional derivative of u of order γ in Riemann-Liouville sense with the generalized Mittag-Leffler kernel is given as [14]:

$$^{FFM}{}_aD_t^{\gamma,\theta}u(t) = \frac{AB(\gamma)}{1-\gamma}\frac{d}{dt^\theta}\int_a^t u(y)E_\gamma\left(\frac{-\gamma}{1-\gamma}(t-y)^\gamma\right)dy, \quad 0<\gamma,\theta\leqslant 1, \tag{1}$$

where $AB(\gamma) = 1-\gamma+\frac{\gamma}{\Gamma(\gamma)}$.

Definition 0.2. Suppose that $u(t)$ is continuous in (a,b). Then the fractal-fractional integral of u with order γ is presented as [14]:

$$^{FFM}{}_0I_t^{\gamma,\theta}u(t) = \frac{\theta\gamma}{AB(\gamma)\Gamma(\gamma)}\int_0^t y^{\theta-1}u(y)(t-y)^{\gamma-1}dy + \frac{\theta(1-\gamma)t^{\theta-1}}{AB(\gamma)}u(t). \tag{2}$$

* Corresponding author.
E-mail addresses: aliakgul00727@gmail.com, aliakgul@siirt.edu.tr (A. Akgül).

https://doi.org/10.1016/j.rinp.2020.103663
Received 3 November 2020; Received in revised form 24 November 2020; Accepted 25 November 2020
Available online 19 December 2020

Formulation of the model

The representation of the constituents of the human population is defined as $S(t)$ (describes the susceptible humans who shall have the maximum probability to catch the fatal virus), $I(t)$ (denotes the infected humans who have convicted with virus) and $R(t)$ (denotes the recovered humans who have healthier due to their internal level of immunity). The physical interpretation of the model has been given as follows: a (describes the normal birth rate of humans), c (represented the convex incidence rate of humans interaction), δ (denotes the death rate of infected humans with virus), α (represented the rate of recovery again become susceptible), μ (the rate at which humans die to other diseases), β (the rate of recovery of humans due to quarantine) and b (the rate of infected immigrant). We present the model of the differential equations as:

$$S'(t) = a - cS(t)I(t)(1+\gamma I(t)) - \mu S(t) + \alpha R(t), \quad \forall t \geqslant 0, \tag{3}$$

$$I'(t) = cS(t)I(t)(1+\gamma I(t)) - (\beta+\mu+\delta-b)I(t), \quad \forall t \geqslant 0, \tag{4}$$

$$R'(t) = \beta I(t) - (\alpha+\mu)R(t), \quad \forall t \geqslant 0. \tag{5}$$

It is clear that, the identity $N(t) = S(t) + I(t) + R(t)$ is fulfilled at all the time $t \geqslant 0$ with the following initial conditions

$$S_0 = S(0), \quad I_0 = I(0), \quad R_0 = R(0). \tag{6}$$

We consider the fractal fractional derivatives and obtain:

$$^{FFM}{}_aD_t^{\gamma,\theta}S(t) = a - cS(t)I(t)(1+\gamma I(t)) - \mu S(t) + \alpha R(t), \quad \forall t \geqslant 0, \tag{7}$$

$$^{FFM}{}_aD_t^{\gamma,\theta}I(t) = cS(t)I(t)(1+\gamma I(t)) - (\beta+\mu+\delta-b)I(t), \quad \forall t \geqslant 0, \tag{8}$$

$$^{FFM}{}_aD_t^{\gamma,\theta}R(t) = \beta I(t) - (\alpha+\mu)R(t), \quad \forall t \geqslant 0. \tag{9}$$

Equilibria of the model

We define corona free equilibria as:

$$(CFE) = C_1 = (S^1, I^1, R^1) = \left(\frac{a}{\mu}, 0, 0\right). \tag{10}$$

We present the corona existing equilibria as:

$$(CEE) = C_2 = (S^*, I^*, R^*). \tag{11}$$

We obtain S^*, I^*, R^* as:

$$S^* = \frac{(\alpha-\beta-\mu-\delta+b)+\alpha\beta I^*}{\mu(\alpha+\mu)}, \tag{12}$$

$$I^* = \frac{-(cB+c\gamma A)+\sqrt{(cB+c\gamma A)^2-4(c\gamma B)(\mu-c_1)}}{2c\gamma B}, \tag{13}$$

$$R^* = \frac{\beta I^*}{\alpha+\mu}, \tag{14}$$

where

$$A = \frac{\alpha-\beta-\mu-\delta+b}{\mu}, \quad B = \frac{\alpha\beta}{\mu(\alpha+\mu)}, \quad c_1 = \beta+\mu+\delta-b. \tag{15}$$

Notice that the reproduction number R_0 is the spectral radius of $A \times B^{-1}$, where A and B are the transmission and transition matrices respectively, obtained from the system (1) to (3) by substituted the corona free equilibria of the model as follows:

$$A = \begin{bmatrix} \frac{ca}{\mu} & 0 \\ 0 & 0 \end{bmatrix} \tag{16}$$

and

$$B = \begin{bmatrix} \beta+\mu+\delta-b & 0 \\ 0 & \alpha+\mu \end{bmatrix} \tag{17}$$

More exactly, notice that

$$R_0 = \frac{ac}{\mu(\mu+\beta+\delta-b)}. \tag{18}$$

Local stability

In this section, we impose the well-posed theorems at the equilibria of the model as follows:

Theorem 0.3. *The corona free equilibrium $C_1 = (S^1, I^1, R^1) = (\frac{a}{\mu}, 0, 0)$ of model is locally asymptotically stable if $R_0 < 1$, otherwise unstable for $R_0 > 1$.*

Proof. The corona-free equilibrium $C_1 = (S^1, I^1, R^1) = (\frac{a}{\mu}, 0, 0)$ is locally asymptotically stable (LAS) if all the eigenvalues, $\lambda_i, \quad i = 1, 2, 3$ where $\lambda_i < 0$ with condition $|\arg(\lambda_i)| > \frac{\alpha\pi}{2}$. For the eigen values, the Jacobean matrix at $C_1 = (\frac{a}{\mu}, 0, 0)$ is obtained as follows:

$$J(C_1) = \begin{bmatrix} -\mu & -\frac{a}{\mu} & \alpha \\ 0 & \frac{a}{\mu}-(\beta+\mu+\delta-b) & 0 \\ 0 & \beta & -(\alpha+\mu) \end{bmatrix} \tag{19}$$

Notice that, the eigenvalue is as, $\lambda_1 = -\mu < 0$,

$$|J(C_1)-\lambda I| = \begin{vmatrix} \frac{a}{\mu}-(\beta+\mu+\delta-b)-\lambda & 0 \\ \beta & -(\alpha+\mu)-\lambda \end{vmatrix} \tag{20}$$

$$\lambda_2 = \frac{a}{\mu}-(\beta+\mu+\delta-b) < 0, \quad \text{if } R_0 < 1, \tag{21}$$

$$\lambda_3 = -(\alpha+\mu) < 0, \tag{22}$$

Hence, all eigenvalues are negative, the given equilibria, C_1 is locally asymptotical stable. □

Theorem 0.4. *The corona existing equilibrium $C_2 = (S^*, I^*, R^*)$ of model is locally asymptotically stable if $R_0 > 1$, otherwise unstable for $R_0 < 1$.*

Proof. The corona existing equilibrium $C_2 = (S^*, I^*, R^*)$ is locally asymptotically stable (LAS) if all the eigenvalues, $\lambda_i, i = 1, 2, 3$ where $\lambda_i < 0$ with condition $|\arg(\lambda_i)| > \frac{\alpha\pi}{2}$. For the eigen values, the Jacobean matrix at $C_2 = (S^*, I^*, R^*)$ is obtained as follows:

$$J(C_2) = \begin{bmatrix} -CI^*(1+rI^*)-\mu & -CS^*-2CS^*rI^* & \alpha \\ CI^*(1+rI^*) & CS^*+2CrS^*I^*-(\beta+\mu+\delta-b) & 0 \\ 0 & \beta & -(\alpha+\mu) \end{bmatrix} \tag{23}$$

$$|J(C_2)-\lambda I| = \begin{vmatrix} -a_1-\mu-\lambda & -a_2 & \alpha \\ a_1 & a_2-a_4-\lambda & 0 \\ 0 & \beta & -a_3-\lambda \end{vmatrix} \tag{24}$$

Then, we obtain

$$\lambda^3 + (a_1-a_2+a_3+a_4+\mu)\lambda + (a_1a_3+a_1a_4-a_2a_3+a_3a_4+a_3\mu-a_2\mu+a_4\mu)\lambda$$
$$+a_1a_3a_4-a_2a_3\mu+a_3a_4\mu-a_1\alpha\beta = 0.$$

Where, $a_1 = CI^*(1+rI^*)$, $a_2 = CS^* + 2CrS^*I^*$, $a_3 = (\alpha+\mu)$, $a_4 = (\beta+\mu+\delta-b)$. By using the Routh-Hurwitz Criterion of 3*rd* order polynomial, we get

$$(a_1-a_2+a_3+a_4+\mu) > 0, \quad (a_1a_3a_4-a_2a_3\mu+a_3a_4\mu-a_1\alpha\beta) > 0, \quad \text{if } R_0 > 1,$$

and

$$(a_1-a_2+a_3+a_4+\mu)(a_1a_3a_4-a_2a_3\mu+a_3a_4\mu-a_1\alpha\beta)$$
$$>(a_1a_3+a_1a_4-a_2a_3+a_3a_4+a_3\mu-a_2\mu+a_4\mu),\quad \text{if}\quad R_0>1,$$

Thus, we have concluded that all eigenvalues are negative and by Routh Hurwitz criteria, the given equilibria, C_2 is locally asymptotical stable. □

Global stability

Theorem 0.5. *For the system (2.1–2.3), the Corona free equilibria C_1 is globally asymptotically stable if $R_0<1$.*

Proof. By using the comparison theorem as presented in [15], the rate of change of the variables (I,R) of system (2.1–2.3) could be rewritten as follows:

$$\begin{pmatrix} I \\ R \end{pmatrix} = (A-B)\begin{pmatrix} I \\ R \end{pmatrix} - \left(1-\frac{\mu}{a}S\right)A\begin{pmatrix} I \\ R \end{pmatrix} \tag{25}$$

where, A and B are defined in subSection 2.1. Since $S\leqslant\frac{a}{\mu},\forall t\geqslant 0$ in region Γ. Then, we get

$$\begin{pmatrix} I \\ R \end{pmatrix} \leqslant (A-B)\begin{pmatrix} I \\ R \end{pmatrix} \tag{26}$$

Since the Eigen values of the matrix $A-B$ all have negative real parts (this comes from the local Theorem 3.1). Then the system (2.1–2.3) is stable, whenever $R_0<1$. So, $(I,R)\rightarrow(0,0)$ as $t\rightarrow\infty$. By the comparison Theorems 2.1–2.3, it follows that $(I,R)\rightarrow(0,0)$ and $S\rightarrow\frac{a}{\mu}$ as $t\rightarrow\infty$. The $(S,I,R)\rightarrow C_1$ as $t\rightarrow\infty$. So, C_1 is globally asymptotically stable for $R_0<1$. □

Theorem 0.6. *The Corona existing equilibrium $(CEE), C_2=(S^*,I^*,R^*)$ is globally asymptotically stable if $R_0>1$.*

Proof. Consider the Lyapunov function as follows [16]:

$$L(t)=A_1\left(S-S^*-S^*\ln\left(\frac{S}{S^*}\right)\right)+A_2\left(I-I^*-I^*\ln\left(\frac{I}{I^*}\right)\right)+A_3\left(R-R^*-R^*\ln\left(\frac{R}{R^*}\right)\right), \tag{27}$$

□

$$\begin{aligned}
{}_a^{FFM}D_t^{r^*,\theta}L(t) = {} & A_1\left(1-\frac{S^*}{S}\right){}_a^{FFM}D_t^{r^*,\theta}S(t)+A_2\left(1-\frac{I^*}{I}\right){}_a^{FFM}D_t^{r^*,\theta}I(t)\\
& +A_3\left(1-\frac{R^*}{R}\right){}_a^{FFM}D_t^{r^*,\theta}R(t)\\
= {} & A_1\left(1-\frac{S^*}{S}\right)[a-cSI(1+rI)-\mu S+\alpha R]\\
& +A_2\left(1-\frac{I^*}{I}\right)[SI(1+rI)-(\beta+\mu+\delta-b)I]\\
& +A_3\left(1-\frac{R^*}{R}\right)[I-(\alpha+\mu)R]\\
= {} & A_1(S-S^*)[a/S-cI(1+rI)-\mu+\alpha R/S]\\
& +A_2(I-I^*)[cS(1+rI)-(\beta+\mu+\delta-b)]\\
& +A_3(R-R^*)[I/R-(\alpha+\mu)].
\end{aligned}$$

By using, $\alpha+\mu=\beta\frac{I}{R^*},\beta+\mu+\delta-b=cS(1+rI^*),\mu=\frac{a}{S^*}-cI^*(1+rI^*)+\alpha\frac{R}{S^*}$, we obtain

$$\begin{aligned}
{}_a^{FFM}D_t^{r^*,\theta}L(t) = {} & -\frac{aA_1(S-S^*)^2}{SS^*}-A_1c(S-S^*)[I(1+rI)-I^*(1+rI^*)]\\
& -\frac{\alpha RA_1(S-S^*)^2}{SS^*}+A_2cSr(I-I^*)^2-A_3\frac{\beta I}{RR^*}(R-R^*)^2.
\end{aligned}$$

We chose $A_1=A_2=A_3=1$, then we obtain

$$\begin{aligned}
{}_a^{FFM}D_t^{r^*,\theta}L(t) = {} & -\frac{a(S-S^*)^2}{SS^*}-c(S-S^*)(I-I^*)-c(S-S^*)r(I-I^*)^2\\
& -\frac{\alpha R(S-S^*)^2}{SS^*}+cSr(I-I^*)^2-\frac{\beta I(R-R^*)^2}{RR^*}\\
= {} & -\frac{a(S-S^*)^2}{SS^*}-c(S-S^*)(I-I^*)-\frac{\alpha RA_1(S-S^*)^2}{SS^*}\\
& -cSr(I-I^*)^2\left(\frac{(S-S^*)(I+I^*)}{S(I-I^*)}-1\right)-\frac{\beta I}{RR^*}(R-R^*)^2\leqslant 0.
\end{aligned}$$

${}^{aFFM}D_t^{r^*,\theta}L(t)\leqslant 0$, for $R_0>1$, and ${}_a^{FFM}D_t^{r^*,\theta}L(t)=0$, only if $S=S^*$, $I=I^*$, $R=R^*$. Therefore, by Lasalle's invariance principle, C_2 is globally asymptomatically stable (G.A.S) in Γ.

Main results

We consider the following problem:

$$\begin{aligned}
{}^{FFM}{}_aD_t^{\gamma,\theta}S(t) &= a-cS(t)I(t)(1+\gamma I(t))-\mu S(t)+\alpha R(t), \quad \forall t\geqslant 0,\\
{}^{FFM}{}_aD_t^{\gamma,\theta}I(t) &= cS(t)I(t)(1+\gamma I(t))-(\beta+\mu+\delta-b)I(t), \quad \forall t\geqslant 0,\\
{}^{FFM}{}_aD_t^{\gamma,\theta}R(t) &= \beta I(t)-(\alpha+\mu)R(t), \quad \forall t\geqslant 0.
\end{aligned}$$

For simplicity, we define

$$\begin{aligned}
K(t,S,I,R) &= \theta t^{\theta-1}(a-cS(t)I(t)(1+\gamma I(t))-\mu S(t)+\alpha R(t))\\
L(t,S,I,R) &= \theta t^{\theta-1}(cS(t)I(t)(1+\gamma I(t))-(\beta+\mu+\delta-b)I(t))\\
M(t,S,I,R) &= \theta t^{\theta-1}(\beta I(t)-(\alpha+\mu)R(t))
\end{aligned}$$

Then, we get

$$\begin{aligned}
\frac{AB(\alpha)}{1-\gamma}\frac{d}{dt}\int_0^t S(\tau)E_\alpha\left(\frac{-\gamma}{1-\gamma}(t-\tau)^\gamma\right)d\tau &= K(t,S,I,R)\\
\frac{AB(\alpha)}{1-\gamma}\frac{d}{dt}\int_0^t I(\tau)E_\alpha\left(\frac{-\gamma}{1-\gamma}(t-\tau)^\gamma\right)d\tau &= L(t,S,I,R)\\
\frac{AB(\alpha)}{1-\gamma}\frac{d}{dt}\int_0^t R(\tau)E_\alpha\left(\frac{-\gamma}{1-\gamma}(t-\tau)^\gamma\right)d\tau &= M(t,S,I,R)
\end{aligned}$$

Applying the AB integral gives,

$$\begin{aligned}
S(t)-S(0) &= \frac{1-\gamma}{AB(\gamma)}K(t,S,I,R)+\frac{\gamma}{AB(\gamma)\Gamma(\gamma)}\int_0^t(t-\tau)^{\gamma-1}K(\tau,S,I,R)d\tau\\
I(t)-I(0) &= \frac{1-\gamma}{AB(\gamma)}L(t,S,I,R)+\frac{\gamma}{AB(\gamma)\Gamma(\gamma)}\int_0^t(t-\tau)^{\gamma-1}L(\tau,S,I,R)d\tau\\
R(t)-R(0) &= \frac{1-\gamma}{AB(\gamma)}M(t,S,I,R)+\frac{\gamma}{AB(\gamma)\Gamma(\gamma)}\int_0^t(t-\tau)^{\gamma-1}M(\tau,S,I,R)d\tau
\end{aligned}$$

We discretize these equations at t_{n+1} as:

$$
\begin{aligned}
S^{n+1} = {} & S^0 + \frac{1-\gamma}{AB(\gamma)} K(t_{n+1}, S^n, I^n, R^n) \\
& + \frac{\gamma}{AB(\gamma)\Gamma(\gamma)} \int_0^{t_{n+1}} (t_{n+1}-\tau)^{\gamma-1} K(\tau, S, I, R) d\tau \\
I^{n+1} = {} & I^0 + \frac{1-\gamma}{AB(\gamma)} L(t_{n+1}, S^n, I^n, R^n) \\
& + \frac{\gamma}{AB(\gamma)\Gamma(\gamma)} \int_0^{t_{n+1}} (t_{n+1}-\tau)^{\gamma-1} L(\tau, S, I, R) d\tau \\
R^{n+1} = {} & R^0 + \frac{1-\alpha}{AB(\alpha)} M(t_{n+1}, S^n, I^n, R^n) \\
& + \frac{\gamma}{AB(\gamma)\Gamma(\gamma)} \int_0^{t_{n+1}} (t-\tau)^{\gamma-1} M(\tau, S, I, R) d\tau
\end{aligned}
$$

Then, we obtain

$$
\begin{aligned}
S^{n+1} = {} & S^0 + \frac{1-\gamma}{AB(\gamma)} K(t_{n+1}, S^n, I^n, R^n) \\
& + \frac{\gamma}{AB(\gamma)} \sum_{j=0}^{n} \left[\frac{h^\gamma K(t_j, S^n, I^n, R^n)}{\Gamma(\gamma+2)} ((n+1-j)^\gamma (n-j+2+\gamma) - (n-j)^\gamma (n-j+2+2\gamma)) \right] \\
& - \frac{\gamma}{AB(\gamma)} \sum_{j=0}^{n} \left[\frac{h^\gamma K(t_{j-1}, S^{n-1}, I^{n-1}, R^{n-1})}{\Gamma(\gamma+2)} \left((n+1-j)^{\gamma+1} - (n-j)^\gamma (n-j+1+\gamma)\right) \right] \\
I^{n+1} = {} & I^0 + \frac{1-\gamma}{AB(\gamma)} L(t_{n+1}, S^n, I^n, R^n) \\
& + \frac{\gamma}{AB(\gamma)} \sum_{j=0}^{n} \left[\frac{h^\gamma L(t_j, S^n, I^n, R^n)}{\Gamma(\gamma+2)} ((n+1-j)^\gamma (n-j+2+\gamma) - (n-j)^\gamma (n-j+2+2\gamma)) \right] \\
& - \frac{\gamma}{AB(\gamma)} \sum_{j=0}^{n} \left[\frac{h^\gamma L(t_{j-1}, S^{n-1}, I^{n-1}, R^{n-1})}{\left((n+1-j)^{\gamma+1} - (n-j)^\gamma (n-j+1+v)\right)} \right] \\
R^{n+1} = {} & R^0 + \frac{1-\gamma}{AB(\gamma)} M(t_{n+1}, S^n, I^n, R^n) \\
& + \frac{\gamma}{AB(\gamma)} \sum_{j=0}^{n} \left[\frac{h^\gamma M(t_j, S^n, I^n, R^n)}{\Gamma(\gamma+2)} ((n+1-j)^\gamma (n-j+2+\gamma) - (n-j)^\gamma (n-j+2+2\gamma)) \right] \\
& - \frac{\gamma}{AB(\gamma)} \sum_{j=0}^{n} \left[\frac{h^\gamma M(t_{j-1}, S^{n-1}, I^{n-1}, R^{n-1})}{\Gamma(\gamma+2)} \left((n+1-j)^{\gamma+1} - (n-j)^\gamma (n-j+1+\gamma)\right) \right]
\end{aligned}
$$

by the method using in [17].

Numerical simulations

For the numerical simulations at disease free state we consider the following values of parameters involved in the system under study, $a = 0.5, \mu = 0.5, \delta = 0.05, b = 0.205, \beta = 0.09871, c = 0.380, \gamma = 0.0003$, $\alpha = 0.854302$. The graphical solution at endemic equilibrium state, we consider the following values, $a = 0.5, \mu = 0.5, \delta = 0.05, b = 0.205, \beta = 0.09871, c = 0.580, \gamma = 0.0003, \alpha = 0.854302$.

In Figs. 1–3, we represent the graphical solutions to the COVID-19 model with the proposed numerical method. All the trajectories adapt the same pattern and converge to the true endemic equilibrium point. In Fig. 1, every trajectory against a specific value of γ with $\theta = 0.96$ shows the disease dynamics of the susceptible individuals. It is easy to notice that each graph in the Fig. 1 has a different rate of convergence (according to γ) but destination of each curve in the steady state. Similarly, the Fig. 2 describes the graphical solutions to the infected individuals. The four curved lines show the behavior of the infected individuals during the course of disease dynamics. It is noteworthy that all the four graphical lines advance towards the true endemic equilibrium point but the rate of convergent to reach at the designed points is different. Also, the curve against the small value of γ converges fastly as compared to the other curves for greater value of γ. So, it is important to mention that γ plays a decisive role in the rate of convergent and ultimately in describing the disease dynamics. The Fig. 3 is the graphical representation of the recovered individuals for the proposed method. All the four sketches in the figure highlight the numerical behavior of the recovered individuals at endemic equilibrium point. The path followed by each curve clarifies the disease dynamics adopted by the recovered populace. Furthermore, each curve reaches at its true converging point i.e. the endemic equilibrium point with different speeds. The different rates of convergence followed by each path is in line with the theoretical results of the fractional calculus.

Now, the Figs. 4–6 bring some influential facts about the numerical solutions at disease free equilibrium point into lime light. Particularly, the Fig. 4 reflects that every graph touches the true equilibrium point. Furthermore, each graph has its own rate to reach at the desired point. This rate of convergence is under the influence of γ, the order of derivative. The Fig. 5 is the graphical representation of the numerical solutions calculated with the help of proposed scheme. All the four graphs touch the disease free steady state at the right point i.e. disease free. It is evident from the graphs that each graph has its own rate of convergence according to the value given to γ. So, the value of γ is helpful in deciding the rate of convergence. One can adjust the disease dynamics by suitably selecting the value of γ. The Fig. 6 validates that all the graphs converge to the desired steady state. Also, these curves depict the dynamics followed by the recovered individuals to reach at the disease free point. Every curve has a specific pace to reach at required disease free point. Also, the different graphs in the Fig. 6 implicate that the disease dynamics of COVID-19 can be synchronized numerically by adjusting an appropriate value of γ.

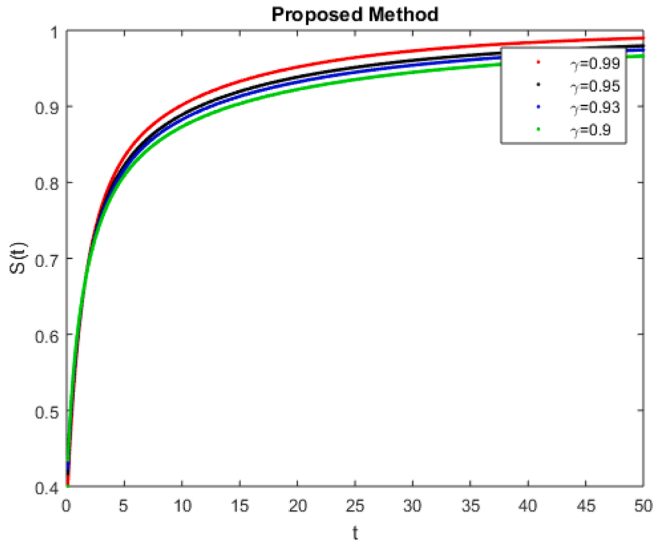

Fig. 1. Numerical simulation for different values of γ with $\theta = 0.96$.

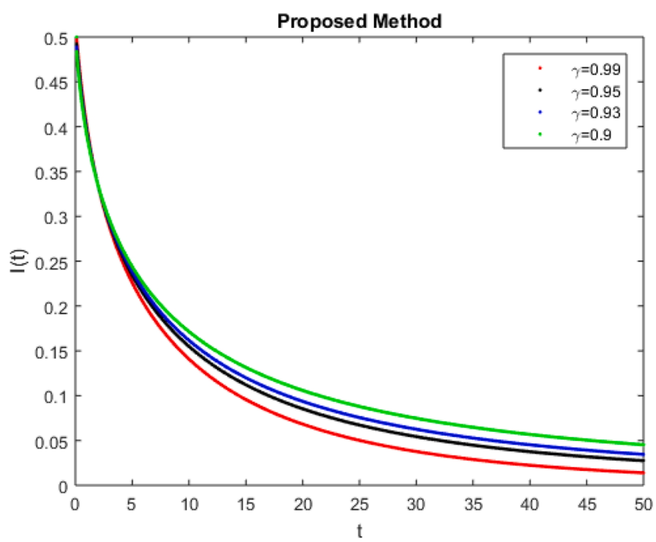

Fig. 2. Numerical simulation for different values of γ with $\theta = 0.96$.

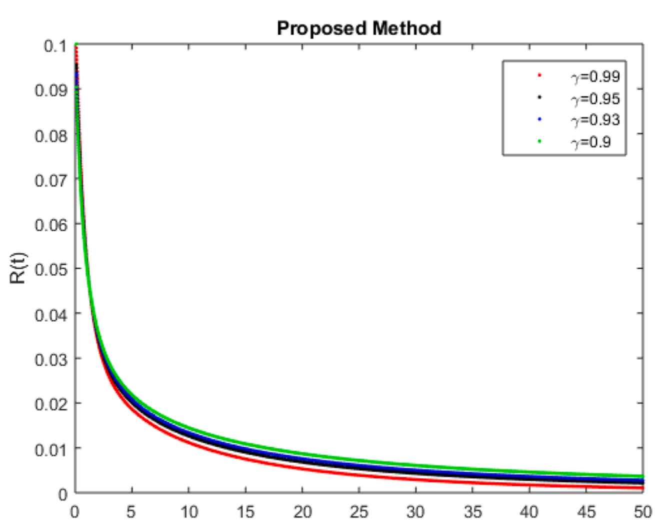

Fig. 3. Numerical simulation for different values of γ with $\theta = 0.96$.

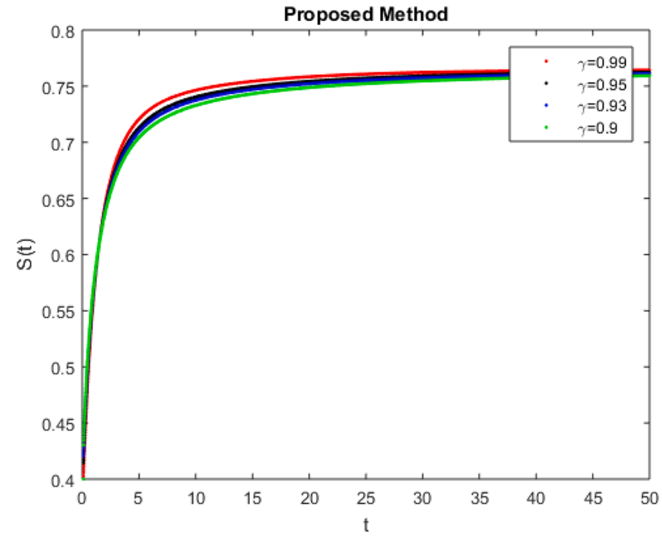

Fig. 4. Numerical simulation for different values of γ with $\theta = 0.96$.

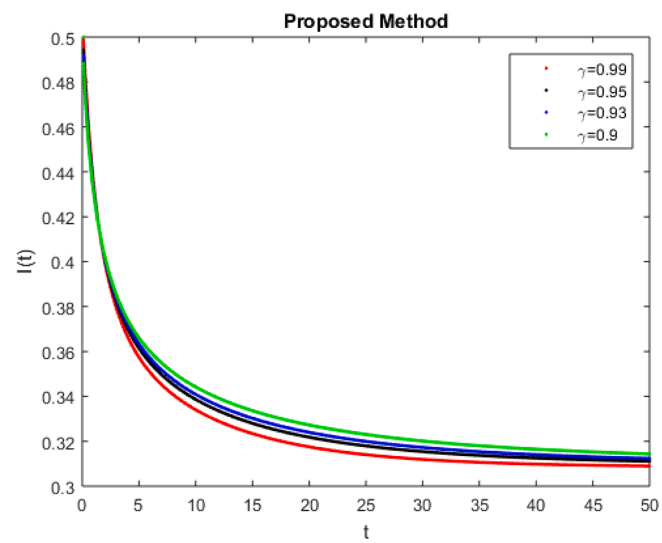

Fig. 5. Numerical simulation for different values of γ with $\theta = 0.96$.

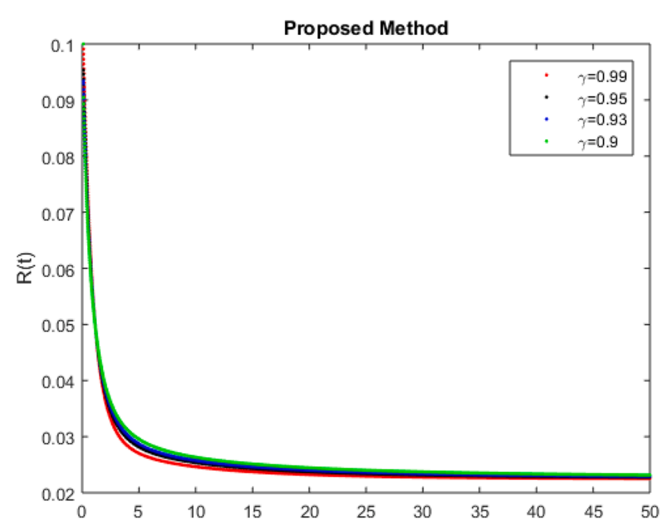

Fig. 6. Numerical simulation for different values of γ with $\theta = 0.96$.

Conclusion

In this work, a mathematical model related to the Covid-19 was enhanced and its different features containing the local and global stability analysis of the diseases free and endemic equilibrium points were presented. Numerical simulations for verification of the global stability analysis of the steady state points were constructed. We used the Mittag-Leffler kernels in the proposed model. We obtained very effective results which will be useful for researchers in their future works.

Author contributions

Conceptualization, A. A. and N. A.; Methodology, A. R.; Software, Z. I.; Validation, M. R., D. B. and M. A. R.; Formal Analysis, A.A.; Investigation, A. A.; Resources, N.A.; Data Curation, M. A. R.; Writing-Original Draft Preparation, A. A.; Writing Review and Editing, N. A.; All authors have read and agreed to the published version of the manuscript.

Declaration of Competing Interest

The authors declare that they have no known competing financial interests or personal relationships that could have appeared to influence the work reported in this paper.

References

[1] Anderson R, May R. Infectious disease of humans, dynamicsand control. Oxford, UK: Oxford University Press; 1995.
[2] Mahdy AMS, Higazy M, Gepreel KA, El-dahdouh AAA. Optimal control and bifurcation diagramfor a model nonlinear fractional SIRC. Alexandria Eng J 2020.
[3] Gorenflo R, Mainardi F. Fractional calculus. In: Fractals and fractional calculus in continuum mechanics. Springer; 1(997): 223–276.
[4] Kilbas A, Srivastava H, Trujillo JJ. Theory and applications of the fractional differential equations, 204, Elsevier (North- Holland), Amsterdam Amsterdam; 2006.
[5] Podlubny I. Fractional differential equations, to methods of their solution and some of their applications. Fractional differential equations: an introduction to fractional derivatives. San Diego, CA: Academic Press; 1998.
[6] Machado JT, Kiryakova V, Mainardi F. Recent history of fractional calculus. Commun Nonlinear Sci Numer Simul 2011;16(3):1140–53.
[7] Kumar S, Cao J, Abdel-Aty M. A novel mathematical approach of COVID-19 with non-singular fractional derivative. Chaos Solitons Fractals 2020;139:110048.s.
[8] Baleanu D, Mohammadi H, Rezapour S. A fractional differential equation model for the COVID-19 transmission by using the Caputo-Fabrizio derivative. Adv Differ Eqs 2020;2020:29.
[9] Kandeil A, Shehata MM, Shesheny RE, Gomaa MR, Ali MA, Kayali G. Complete genome sequence of middle east respiratory syndrome coronavirus isolated from a dromedary camel in Egypt. Genome Announc 2016.
[10] Kucharski AJ, Russell TW, Diamond C, Liu Y, Edmunds J, Funk S, Eggo RM, Sun F, Jit M, Munday JD, Davies N, Gimma A, van Zandvoort K, Gibbs H, Hellewell J, Jarvis CI, Clifford S, Quilty BJ, Bosse NI, Abbott S, Klepac P, Flasche S. Early dynamics of transmission and control of COVID-19: a mathematical modelling study. Lancet Infect Dis; 2020.
[11] Lam TTY, Shum MHH, Zhu HC, Tong YG, Ni XB, Liao YS, Wei W, Cheung WYM, Li WJ, Li LF, Leung GM, Holmes EC, Hu YL, Guan Y. Identifying SARS-CoV-2 related coronaviruses in Malayan pangolins. Nature 2020.
[12] Kissler SM, Tedijanto C, Goldstein E, Grad YH, Lipsitch M. Projecting the transmission dynamics of SARS-CoV-2 through the postpandemic period. Science 2020.
[13] Tenreiro Machado JA, Rocha-Neves JM, Andrade JP. Computational analysis of the SARS-CoV-2 and other viruses based on the Kolmogorov's complexity and Shannon's information theories. Nonlinear Dyn 2020.
[14] Atangana A. Fractal-fractional differentiation and integration: connecting fractal calculus and fractional calculus to predict complex, system. Chaos Solitons Fractals 2017;102:396–406.
[15] Lakshmikantham V, Leela S, Martynyuk AA. Stability Analysis of Non-Linear System. New York: Marcel Dekker Inc.; 1989.
[16] Mouaouine A, Boukhouima A, Hattaf K, Yousfi N. A fractional order SIR epidemic model with nonlinear incidence rate. Adv Differ Eqs; 2018.
[17] Toufik M, Atangana A. New numerical approximation of fractional derivative with non-local and non-singular kernel: application to chaotic models. Eur Phys J Plus 132(10); 444.
[18] Akgül A. A novel method for a fractional derivative with non-local and non-singular kernel. Chaos Solitons Fractals 2018;114:478–82.
[19] Akgül EK. Solutions of the linear and nonlinear differential equations within the generalized fractional derivatives. J Nonlinear Sci 2019;29(2):023108.
[20] Owolabi KM, Atangana A, Akgül A. Modelling and analysis of fractal-fractional partial differential equations: Application to reaction-diffusion model. Alexandria Eng J 2020;59:2477–90.
[21] Atangana A, Akgül A, Owolabi KM. Analysis of fractal fractional differential equations. Alexandria Eng J 2020;59:1117–34.
[22] Atangana A, Akgül A. Can transfer function and Bode diagram be obtained from Sumudu transform. Alexandria Eng J 2020;59:1971–84.